NOTE

Magnetic Resonance in Medicine 000:000–000 (2012)

Novel MRI-Compatible Tactile Stimulator for Cortical Mapping of Foot Sole Pressure Stimuli with fMRI

Ying Hao,[1] Brad Manor,[1,2] Jing Liu,[1,3] Kai Zhang,[1] Yufeng Chai,[1] Lewis Lipsitz,[2] Chung-Kang Peng,[2] Vera Novak,[2] Xiaoying Wang,[1,3] Jue Zhang,[1,4]* and Jing Fang[1,4]

Foot sole somatosensory feedback is critical to motor control and declines with aging and disease. To enable study of cortical networks underlying foot sole somatosensation, we developed a pneumatic tactile stimulator capable of producing one degree-of-freedom (DOF) oscillations with preset waveform, frequency (≤10 Hz), force magnitude (5–500 N), duty cycle (20–100%), and contacted surface area over which pressures are applied to the foot sole. Image tests (anatomical/functional/field map) of a phantom demonstrated that the device is compatible with 3 T MRI. Gradient-recalled echo-planar images of seven healthy young adults using a typical block-designed 1 Hz sinusoidal stimulation protocol revealed significant activation contralaterally within the primary somatosensory cortex and paracentral gyrus, and bilaterally within the secondary somatosensory cortex. The stimulation system may therefore serve as a research tool to study functional brain networks involved in the perception and modulation of foot sole somatosensation and its relationship to motor control. Magn Reson Med 000:000–000, 2012. © 2012 Wiley Periodicals, Inc.

Key words: plantar; somatosensory; gait; feedback; pneumatic

Foot sole somatosensation plays a critical role among the active feedback loops that contribute to the control of standing and walking. Aging and disease often impair foot sole somatosensation, and consequently, decrease balance and increase the risk of falling. Still, behavioral research indicates that some older adults with foot sole somatosensory impairment can maintain balance to a similar degree as their healthy counterparts (1). Furthermore, both perceptible and imperceptible foot sole vibratory stimulation during standing (2) and walking (3) reduce movement variability in older adults both with and without movement disorders.

To determine the neural mechanisms underlying these adaptive capacities, we aimed to develop and evaluate an MRI-compatible tactile stimulator capable of applying controlled patterns of pressure to the foot sole. Numerous devices have been developed to study the brain's response to somatosensory stimuli. These devices have focused primarily on the application of low amplitude, high-frequency vibratory stimuli (4–7). With respect to the foot sole, Gallasch et al. (8) successfully mapped somatosensory cortical activation in response to mechanical vibrations (i.e., 20–100 Hz oscillations with an maximum contact force of 20 N) produced by an electrically driven magnetic actuator.

The pressures experienced beneath the foot during weight-bearing activities, however, often meet or exceed one's body weight and may vary considerably in frequency and amplitude. As a critical first step to enable study of the brain's response to this type of stimuli, we have developed an air-driven stimulation system capable of applying relatively high-pressure stimuli to the foot sole with a programmable waveform and adjustable surface area over which the pressure is applied. Combination of this new tool with functional MRI (FMRI) will afford insight into the functional brain networks underlying this source of afferent feedback under different experimental conditions. This experimental paradigm will enable study of the neural circuits underlying foot sole somatosensation and the mechanisms of neural adaptation that optimize behavior in the presence of both acute and chronic alterations to this source of afferent feedback.

MATERIALS AND METHODS

Basic Design of Tactile Stimulation System

The foot sole stimulation system consists of an air compressor, a control unit (i.e., a microprocessor, proportional valve, five-port air-operated valve, and user interface) and an aluminum pneumatic actuator attached to a nonferromagnetic support platform (Fig. 1).

Foot sole pressure stimulation is produced by a linear pneumatic actuator consisting of a single-acting, single-rod air cylinder (CG1BN32-40-XC6, SMC, Tokyo, Japan). This actuator was chosen for several reasons. First, it is comprised of aluminum and driven by air, and therefore nonferromagnetic. Second, it is capable of producing linear output force ranging from 5 to 500 N, and thus, suitable for applications requiring the generation of relatively large pressure stimuli. Third, stroke movement speed is 40–1000 mm/s, and thus, enables rapidly generated pressures to the foot sole.

[1]Academy for Advanced Interdisciplinary Studies, Peking University, Beijing, China.

[2]Department of Medicine, Beth Israel Deaconess Medical Center, Harvard Medical School, Boston, Massachusetts, USA.

[3]Department of Radiology, Peking University First Hospital, Beijing, China.

[4]College of Engineering, Peking University, Beijing, China.

Grant sponsor: National Natural Science Foundation of China; Grant number: 31150110173; Grant sponsor: Fundamental Research Funds for the Central Universities, China; Grant sponsor: MeRIT award from Harvard Catalyst; Grant number: 1KL2RR025757-04; Grant sponsor: NIH; Grant number: KL2 RR 025757.

*Correspondence to: Jue Zhang, Ph.D., Academy for Advanced Interdisciplinary Studies, Peking University, Beijing 100871, People's Republic of China. E-mail: zhangjue@pku.edu.cn

Received 11 July 2011; revised 14 March 2012; accepted 18 April 2012.

DOI 10.1002/mrm.24330
Published online in Wiley Online Library (wileyonlinelibrary.com).

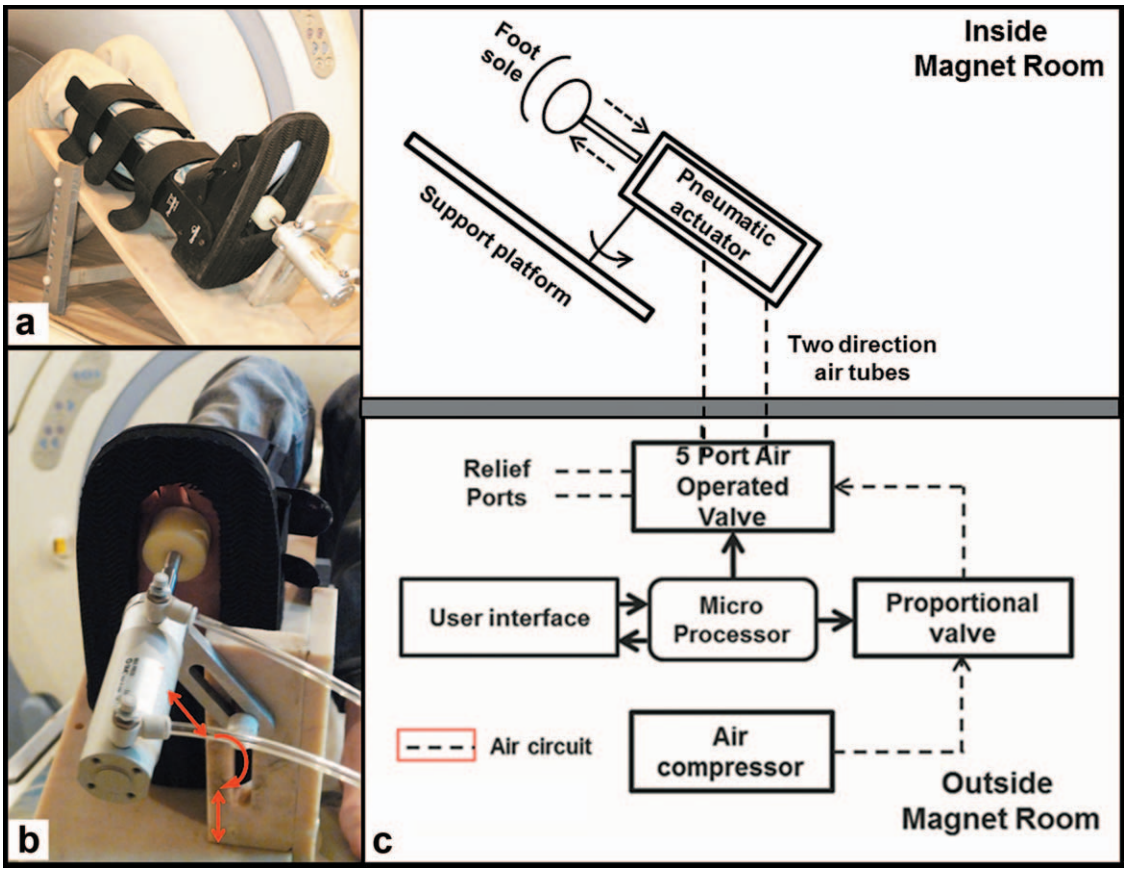

FIG. 1. Foot sole pressure stimulation is applied to the foot by an aluminum pneumatic actuator attached to a support platform (a). The actuator can be adjusted to any location of the foot sole (b). Force generation is regulated by a control unit located outside of the magnet room (c, lower panel) attached to the nonferromagnetic actuator and platform (c, upper panel) via 4-m plastic air tubes. [Color figure can be viewed in the online issue, which is available at wileyonlinelibrary.com.]

The control unit affords independent control of the magnitude and frequency of force application to the foot sole. Specifically, the microprocessor (MSP 430 F168, Texas Instruments, Dallas, TX, USA) controls air flow to the pneumatic actuator by regulating voltage input to two electronic air valves. First, a proportional electropneumatic valve connected to an air compressor enables stepless control of the amount of air flow to the actuator. The relationship between voltage input to the proportional valve and air flow to the actuator is linear (see the following section), thus, enabling precise control of the magnitude of force application to the foot sole. Second, a five-port air-operated valve enables movement direction control of the actuator's cylinder, and thus, the waveform (i.e., the frequency and duty cycle) of force application. Movement direction of the cylinder can be fully reversed in 100 ms, thus, enabling a maximal oscillatory frequency of 10 Hz. The microprocessor also produces a trigger in/out (TTL level) signal to synchronize the system with the MR scanner.

We developed a user interface using C programming, which allows the investigator to program the characteristics of foot stimulation. It consists of a 16-character liquid crystal display (LCD) display and four control buttons: one for selection of predefined waveforms (sine/square/triangle), waveform parameters (frequency/duty cycle/magnitude), and MRI-trigger options; two for up/down regulation of parameters; one for downloading and applying self-programmed stimulation waveforms. Self-programming allows the investigator to set the force output for each 0.02 s increment of one cycle, which can be repeated during stimulation protocols. During stimulation, the magnitude, duty cycle, and frequency of force (as determined by voltage input) are displayed on the LCD screen. All components of the control unit are located outside the scanner room and connected with the actuator inside via plastic air tubes.

A support platform was used to secure the actuator in place during the application of pressure stimulation. A plastic medical boot was modified and attached to a support surface comprised of nonferromagnetic plastic and nylon materials. The support platform was designed to fix the ankle joint at 90° of dorsiflexion yet enable adjustment of knee and hip joint angle. Visual inspection during pilot studies indicated that applying pressure to the foot sole with the knee joint flexed, as opposed to fully extended, reduced translational movements of the head. The actuator was attached to the support platform perpendicularly to the foot sole using a multijoint lever system that enabled anterior–posterior and medial–lateral adjustments relative to the foot. A series of Velcro straps secured the support platform to the scanner table, as well as the subject's foot, shank, and thigh to the support platform.

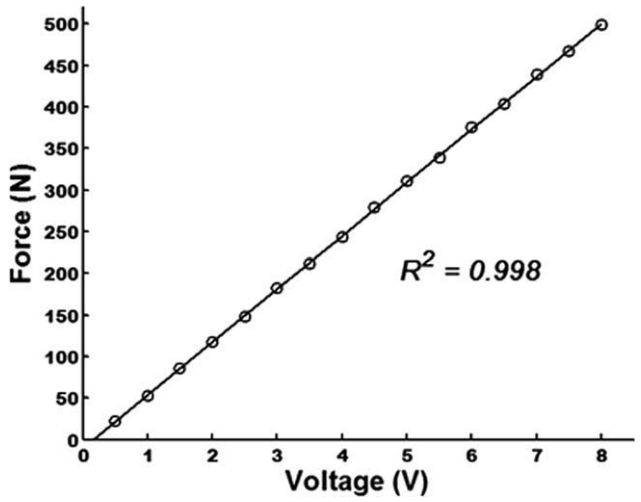

FIG. 2. The relationship between voltage input to the proportional electropneumatic valve on the air compressor and the force output of the actuator on the foot sole.

Implementation, Calibration, and Performance Testing

To determine the relationship between voltage input to the proportional electropneumatic valve on the air compressor and force output of the actuator, an instrumented foot pressure insole (RSscan Lab, Ipswich, Suffolk, UK) was first calibrated inside the magnet room and then placed between the foot sole and the cylinder cover of the actuator. The voltage input–force output relationship, which was tested on five young adult subjects using square waveform inside the magnet room, was highly linear (Fig. 2). At each voltage, the standard deviation about the recorded mean force value was less than 0.47 N. As such, we subsequently used a linear-fit function ($y = 63.833x - 10.164$) to transform voltage into force on the LCD display.

Performance of the stimulation system was then tested with the instrumented pressure insole to measure the actual force produced on the foot sole in response to preprogrammed patterns of stimulation in a single subject inside of the scanner room (Fig. 3). To demonstrate the system's versatility, tested stimulation waveforms included a 1 Hz sine curve with a duty cycle of 80%, a 2

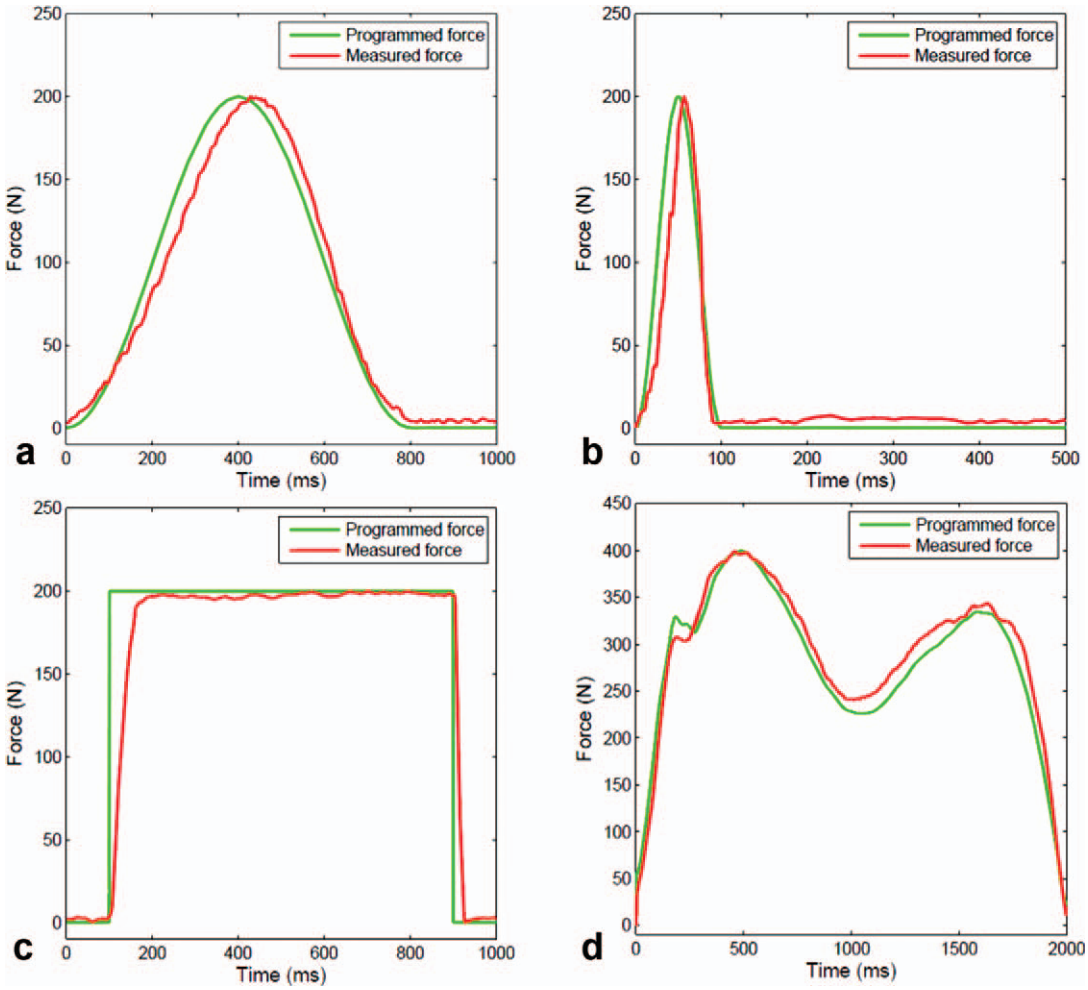

FIG. 3. Foot sole stimulation system performance. We compared four different patterns of preprogrammed foot stimulation (green line) with the actual stimulation applied to the foot sole (red line). Stimulation patterns included (a) a 1 Hz sine curve with an 80% duty cycle, (b) a 2 Hz sine curve with a 20% duty cycle, (c) a square waveform with an 80% duty cycle, (d) a biphasic waveform similar to that experienced by the foot when walking. [Color figure can be viewed in the online issue, which is available at wileyonlinelibrary.com.]

Hz sine curve with a duty cycle of 20%, a square waveform (80% duty cycle), and a biphasic waveform mimicking the typical ground reaction force experienced when walking.

FMRI Compatibility

All of the imaging tests were performed on a 3 T scanner (Signa Excite HD; GE Medical Systems, Milwaukee, WI) with an eight-channel head coil. With the stimulator located 90 cm away from the phantom center (closer than the distance from foot to head), a phantom was imaged under the following conditions: (1) stimulation system powered on; (2) stimulation system powered off; (3) control (i.e., no stimulation system present). Anatomical, functional, and magnetic field map images were acquired under each condition. Acquisition parameters were as follows: (1) anatomical—three-dimensional (3D) fast spoiled gradient echo sequence, pulse repetition time/echo time = 7.8/3.0 ms, flip angle = 20°, inversion time = 450 ms, field of view = 23 × 23 cm^2, slice thick = 2.0 mm with 1-mm overlap, resolution = 1 × 1 mm^2, two measurements. (2) Functional—gradient-recalled echo-planar imaging sequence, pulse repetition time = 2000 ms, echo time = 30 ms, flip angle = 90°, matrix = 64 × 64, thickness/spacing = 4/1 mm, field of view = 23 × 23 cm^2, 28 interleaved axial slices, 30 measurements. (3) Magnetic field map—2D fast spoiled gradient echo sequence, pulse repetition time = 488 ms, echo time-1 = 5.19 ms, echo time-2 = 7.65 ms, flip angle = 60°, field of view = 23 × 23 cm^2, 64 × 64 matrix, 3.0-mm thickness, 1-mm gap, 15 slices.

In addition to a visual inspection of all images for artifacts, region-of-interest (ROI) image quality parameters were calculated for each image type in each condition using SPM8 software (the Wellcome Trust Centre for Neuroimaging, London, United Kingdom) and custom MATLAB (The MathWorks, Inc., Natick, MA) programming. All tests were calculated from a central 30-mm radius circular ROI in the center of the phantom. The signal-to-noise ratio of anatomical images was calculated following the methods delivered by National Electrical Manufacturers Association (9). The signal-to-fluctuation-noise ratio (SFNR) of functional images was calculated by creating a "signal image" from the voxel-wise time-series mean without the first 10 measurements. Then, a fluctuation noise image was formed by detrending the voxel-wise time series with a second-order Legendre polynomial and computing the voxel-wise time-series standard deviation. The signal image was divided by the noise image, and the ROI mean (and standard deviation) of the resulting SFNR image was recorded as the SFNR (10). For the magnetic field maps, the ROI mean and standard deviation were recorded to check for subtle magnetic field perturbations potentially arising from the presence of the device.

The Brain Response to Foot Sole Stimulation

Participants

Seven healthy adults (4M/3F) aged 23–27 years were recruited and signed written informed consent as approved by the local ethical committee. Inclusion criteria were right-foot dominance and the ability to perceive 10 g of pressure at five weight-bearing sites on the right foot sole as determined with a 5.07 gauge Semmes–Weinstein monofilament and standard testing procedures. Exclusion criteria included any acute illness, self-reported history of cardiovascular, metabolic, or neurological disease, musculoskeletal disorders, and previous surgery on the back or lower extremities.

Protocol

A block-design FMRI protocol was completed using gradient-recalled echo-planar imaging sequences with alternating blocks of foot sole stimulation and rest (i.e., no stimulation). Each block was 30 s in duration and repeated three times. With the subject barefoot, foot sole pressure stimulation was applied to a circular area 4 cm in diameter over the head of the first metatarsal of the right foot. Maximum force output of the actuator was set to 10% of the subject's body mass and was applied in a 1 Hz sinusoidal waveform with a duty cycle of 80% (i.e., Fig. 3a).

To determine if larger pressure stimuli would induce motion artifact due to head movement, a subsample (n = 3) completed a block-design protocol in which stimulation was applied in a square waveform (80% duty cycles) with maximum force output set to 40% body mass (i.e., Fig. 3c).

Functional imaging parameters were similar to the phantom test previously described. We acquired 90 volumes with 28 interleaved axial slices covering the entire cerebrum and cerebellum. Following the FMRI protocol, high-resolution structural images of the brain were acquired using the 3D fast spoiled gradient echo sequence above.

Imaging and Statistical Analysis

First, to quantify the extent of head motion induced by high-frequency foot stimulation, SFNR was calculated from white matter (segmented by SPM8) on raw echo-planar imaging images with/without foot stimulation on all seven subjects. Then, functional images were processed by SPM8, images were first realigned to the first scan to correct for potential head movement between scans and then time corrected to compensate for delays associated with acquisition time differences. Six-parameter head motion curves were generated. All images were normalized to a 2 × 2 × 2 mm^3 Montreal Neurological Institute template. Functional images were spatially smoothed using a gaussian filter with the full width/half maximum parameter set to 8 mm and temporally filtered using a cutoff of 128 s. General linear modeling was applied to detect activation patterns for each individual. One sample t tests were then applied to generate a group result on the t-map of each individual (False discovery rate [FDR] $P < 0.05$, at least 10 contiguous voxels).

Table 1
MRI Compatibility Test on Phantom Center ROI

Foot stimulator condition	Anatomic SNR (mean ± SD)	Functional SFNR (mean ± SD)	Field map mean (mean ± SD)
Powered on	80 ± 2	768 ± 71	2013 ± 15
Powered off	81 ± 1	771 ± 66	2018 ± 15
Absent from room	79 ± 1	764 ± 65	2011 ± 15

SNR, signal-to-noise ratio; SFNR, signal-to-fluctuation-noise ratio; SD, standard deviation.

RESULTS

Compatibility of the Foot Sole Stimulation System with 3 T MRI

FMRI compatibility tests using the phantom revealed that the foot sole stimulation system did not affect image quality. Within the tested ROI, the signal-to-noise ratio of anatomic images, the SFNR of functional images, and the mean and standard deviation of the magnetic field maps were virtually identical with the stimulation system present (whether powered on or off) as compared to the stimulation system absent (Table 1).

Cortical Response to Foot Sole Stimulation

Foot sole stimulation did not induce significant motion artifact due to head movement. Average 3D head translation and rotation relative to the first image was less than 1 mm and 1° in all subjects for both sinusoidal stimuli (magnitude = 10% body mass) and square-wave stimuli (magnitude = 40% body mass). The average SFNR value calculated from white matter on the raw echo-planar images was not significantly different ($P = 0.46$) between conditions of no stimulation (135.6 ± 9.4) and stimulation (136.8 ± 7.2). Furthermore, we did not visually detect remarkable motion artifacts or unthresholded statistical parameter maps during data processing.

1 Hz sinusoidal foot sole pressure stimulation resulted in significant cortical activation contralaterally within the primary somatosensory cortex (postcentral gyrus, Brodmann areas 1 and 2) and primary motor cortex (paracentral gyrus, Brodmann area 4). Bilateral activation was observed within the secondary somatosensory cortex (inferior parietal lobule, Brodmann area 40) (FDR $P < 0.05$, $k \geq 10$) (Fig. 4). Cerebellar activation was observed in three of seven subjects (uncorrected $P < 0.001$, $k \geq 10$); however, this activation did not reach significance in the group map.

DISCUSSION

The foot sole stimulation system accurately produces customized pressure waveforms, can be easily adjusted to stimulate different foot sole areas, and does not interfere with image quality. Oscillatory pressure stimulation applied to a portion of the foot sole was associated with a characteristic network of brain activation in healthy young adults. Furthermore, the oscillatory force stimuli of up to 40% of subject body mass did not cause motion artifact due to head movement. This novel system is therefore feasible for FMRI studies conducted at 3 T and can serve as a valuable research tool to study the functional brain networks involved in the perception and modulation of foot sole somatosensation.

As compared to previous MRI-compatible systems designed to apply low-force vibrotactile stimuli, this air-driven device is capable of greater force output, as well as independent control of the force waveform and surface area over which pressure stimulation is applied. As all control elements and ferromagnetic components are located outside of the scanner room, this versatile system will enable researchers to use high-field MRI to study the brain response to an array of customizable foot pressure stimuli.

Our proof-of-concept imaging study demonstrated that 1 Hz sinusoidal-wave pressure stimulation to a relatively small portion of one foot sole produced significant brain activation within regions linked to both somatosensory and motor function. Activation within the left primary somatosensory cortex (Brodmann areas 1 and 2) in response to stimulation of the right foot sole was expected as these regions receive input from both slowly and rapidly adapting cutaneous mechanoreceptors (11,12). Bilateral activation within the secondary

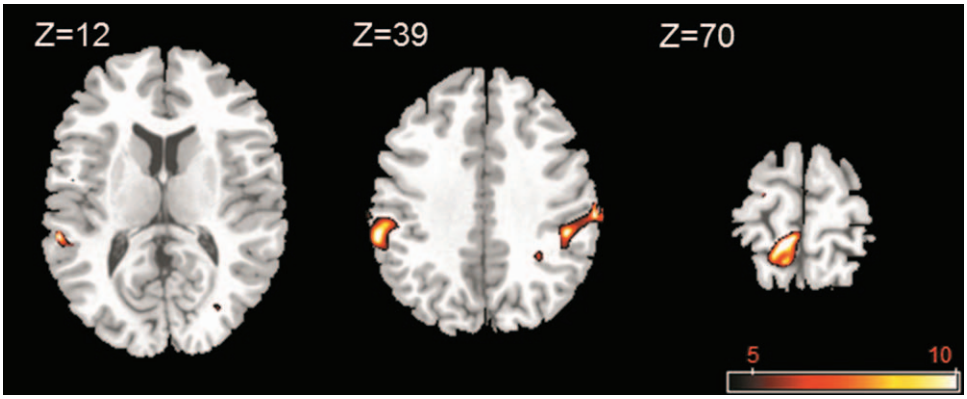

FIG. 4. Group activation clusters overlaid on a standard T_1 template for the contrasts of the images acquired during foot sole stimulation when compared with rest. Stimulation elicited well-pronounced brain activation contralaterally within the primary somatosensory cortex and the primary motor cortex, and bilaterally within the secondary somatosensory cortex. FMRI maps are in standard neurological convention with left = left and right = right.

somatosensory cortex likely stemmed from a combination of feed-forward projections from the primary somatosensory cortex (13) and transcallosal projections to the ipsilateral hemisphere (14). Significant activation within the contralateral primary motor cortex, which has also been reported in response to vibratory foot sole stimulation (15,16), may have been caused by direct thalamocortical proprioceptive projections to the primary motor cortex in response to repetitive stretching of the short muscles within the plantar region of the foot sole (17).

Initial calibration experiments indicated that the voltage input/force output relationship of the stimulation system was linear at a constant frequency. However, under conditions of varying stimulation frequency, eddy currents created by movement of the aluminum actuator cylinder within the magnetic field may interfere with the force output (18). To test this potential effect, separate experiments were conducted inside and outside the scanner. In each setting, a sinusoidal pressure waveform with a peak force of 200 N was applied to the foot sole with an increasing frequency from 1 to 10 Hz. As measured by an instrumented pressure insole, increasing the frequency of oscillation did not affect peak forces outside the magnet room, yet resulted in a small but significant reduction (1.58 N) in peak force production inside the magnet room. This result is consistent with previous research (18) and should therefore be considered when designing protocols. Furthermore, in applications within higher magnetic fields (e.g., 7 T), an actuator constructed of glass and graphite materials may be needed to ensure accuracy of foot stimulation.

In conclusion, the foot sole stimulation system does not interfere with image quality, does not produce motion artifact with applied load, and elicits a reliable pattern of brain activation. Future studies that use multiple, independently controlled pneumatic actuators over larger surface areas to stimulate the soles of both feet may more accurately simulate the pressures experienced when standing and walking and enable study of the functional brain networks involved in this critical source of afferent feedback. Experimental paradigms that combine FMRI imaging of the brain during foot sole stimulation under different conditions with behavioral studies of walking will afford first-of-its-kind insight into the cortical networks underlying the control of this fundamental human behavior in both health and disease.

ACKNOWLEDGMENTS

Ying Hao and Brad Manor are co-first authors to this work. The content is solely the responsibility of the authors and does not necessarily represent the official views of Harvard Catalyst, Harvard University and its affiliated academic health care centers, the National Center for Research Resources, or the National Institutes of Health.

REFERENCES

1. Manor B, Costa MD, Hu K, Newton E, Starobinets O, Kang HG, Peng CK, Novak V, Lipsitz LA. Physiological complexity and system adaptability: evidence from postural control dynamics of older adults. J Appl Physiol 2010;109:1786–1791.
2. Costa M, Priplata AA, Lipsitz LA, Wu Z, Huang NE, Goldberger AL, Peng CK. Noise and poise: enhancement of postural complexity in the elderly with a stochastic-resonance-based therapy. Europhys Lett 2007;77:68008.
3. Novak P, Novak V. Effect of step-synchronized vibration stimulation of soles on gait in Parkinson's disease: a pilot study. J Neuroeng Rehabil 2006;3:9.
4. Golaszewski SM, Siedentopf CM, Baldauf E, Koppelstaetter F, Eisner W, Unterrainer J, Guendisch GM, Mottaghy FM, Felber SR. Functional magnetic resonance imaging of the human sensorimotor cortex using a novel vibrotactile stimulator. Neuroimage 2002;17:421–430.
5. Graham SJ, Staines WR, Nelson A, Plewes DB, McIlroy WE. New devices to deliver somatosensory stimuli during functional MRI. Magn Reson Med 2001;46:436–442.
6. Harrington GS, Wright CT, Downs JR. A new vibrotactile stimulator for functional MRI. Hum Brain Mapp 2000;10:140–145.
7. Stippich C, Hofmann R, Kapfer D, Hempel E, Heiland S, Jansen O, Sartor K. Somatotopic mapping of the human primary somatosensory cortex by fully automated tactile stimulation using functional magnetic resonance imaging. Neurosci Lett 1999;277:25–28.
8. Gallasch E, Golaszewski SM, Fend M, Siedentopf CM, Koppelstaetter F, Eisner W, Gerstenbrand F, Felber SR. Contact force- and amplitude-controllable vibrating probe for somatosensory mapping of plantar afferences with fMRI. J Magn Reson Imaging 2006;24:1177–1182.
9. Association NEM. Determination of signal-to-noise ratio (SNR) in diagnostic magnetic resonance imaging. NEMA standards Publications MS 1-2008. National Electrical Manufacturers Association: Rosslyn; 2008.
10. Friedman L, Glover GH. Report on a multicenter fMRI quality assurance protocol. J Magn Reson Imaging 2006;23:827–839.
11. Kurth R, Villringer K, Curio G, Wolf KJ, Krause T, Repenthin J, Schwiemann J, Deuchert M, Villringer A. fMRI shows multiple somatotopic digit representations in human primary somatosensory cortex. Neuroreport 2000;11:1487–1491.
12. Geyer S, Schleicher A, Zilles K. Areas 3a, 3b, and 1 of human primary somatosensory cortex. Neuroimage 1999;10:63–83.
13. Kany C, Treede RD. Median and tibial nerve somatosensory evoked potentials: middle-latency components from the vicinity of the secondary somatosensory cortex in humans. Electroencephalogr Clin Neurophysiol 1997;104:402–410.
14. Burton H, Videen TO, Raichle ME. Tactile-vibration-activated foci in insular and parietal-opercular cortex studied with positron emission tomography: mapping the second somatosensory area in humans. Somatosens Mot Res 1993;10:297–308.
15. Siedentopf CM, Heubach K, Ischebeck A, Gallasch E, Fend M, Mottaghy FM, Koppelstaetter F, Haala IA, Krause BJ, Felber S, Gerstenbrand F, Golaszewski SM. Variability of BOLD response evoked by foot vibrotactile stimulation: influence of vibration amplitude and stimulus waveform. Neuroimage 2008;41:504–510.
16. Golaszewski SM, Siedentopf CM, Koppelstaetter F, Fend M, Ischebeck A, Gonzalez-Felipe V, Haala I, Struhal W, Mottaghy FM, Gallasch E, Felber SR, Gerstenbrand F. Human brain structures related to plantar vibrotactile stimulation: a functional magnetic resonance imaging study. Neuroimage 2006;29:923–929.
17. Murphy JT, Wong YC, Kwan HC. Afferent–efferent linkages in motor cortex for single forelimb muscles. J Neurophysiol 1975;38:990–1014.
18. Jeneson JA, Schmitz JP, Hilbers PA, Nicolay K. An MR-compatible bicycle ergometer for in-magnet whole-body human exercise testing. Magn Reson Med 2010;63:257–261.